# Hardware Implementation of Various DTC Strategies Using dSpace 1104 for Induction Motor Drive

Abdelkarim Ammar, Amor Bourek, Abdelhamid Benakcha, Tarek Ameid, Younes Azzoug

# Hardware Implementation of Various DTC Strategies Using dSpace 1104 for Induction Motor Drive

Abdelkarim AMMAR*, Amor BOUREK, Abdelhamid BENAKCHA, Tarek AMEID and Younes AZZOUG
Electrical engineering Laboratory of Biskra LGEB, University of Mohammed Khider Biskra, Algeria

## Keywords

«Induction Motor (IM)», «Direct Torque Control (DTC)», «Switching Table», «Space Vector Modulation (SVM)», «dSpace 1104».

## Abstract

This paper presents different enhancement techniques of basic direct torque control strategy for induction motor drive. It is well-known that the conventional DTC suffers from high torque ripples and variable switching frequency due to utilizing hysteresis comparators and lookup switching table. In this paper two improved techniques are presented. The first one deal with the use of an extended switching table which divides the flux locus into twelve sectors instead of six in order to solve control ambiguity and reduce ripples. The second technique bases on replacing the switching table by space vector modulation in order to maintain a fixed switching frequency and to minimize consequently the high torque and flux ripples. The effectiveness of the presented algorithms is investigated by an experimental implementation with the aid of real-time interface (RTI) based on dSpace 1104 bored.

## I. Introduction

The Direct Torque Control (DTC) was presented in the middle of the 80s. This strategy was an alternative to the field oriented control (FOC). It bases on the direct selecting of the switching states to control the voltage source inverter (VSI) through a switching look-up table [1].DTC offers more advantages compared to FOC like: simpler scheme, faster response and less dependence to machine parameters. The control of stator flux and torque is done by hysteresis controllers which choose the input voltage vector according to flux and torque errors.

However, the main problems of this method are the high ripples and the variable switching frequency, they lead to an acoustical noise and decrease the performances of the controlled machine. In order to overcome these problems and improve the performances of DTC, various proposed solutions have been presented, such as multilevel converters, artificial intelligence techniques, switching table modification and space vector modulation (SVM) [2]–[4]. The twelve sector DTC uses twelve-sector divisions in (α, β) plan instead of the usual plane divisions of six sectors [5]. This modification provides a new extended switching table which can solve the ambiguity in voltage vectors selection. Moreover, it has a slight effect on reducing ripples and harmonics and offers better dynamic in high and low speed regions [6].

The fixed switching frequency based DTC was introduced in many works also [7], [8]. The main difference between the classical and the SVM based DTC strategies is replacing the switching table by the space vector modulation for inverter states generation. In each sampling period, SVM preserves a constant switching frequency which can reduce considerably torque/flux ripples. Serval SVM-DTC methods have been proposed according to their structure, we mention among of them the stator filed oriented direct torque control (SFOC-DTC) based on linear PI controllers [9]. Another technique is known by the closed loop torque control or load angle control [10]. This later offers a simpler design in the stationary frame ($\alpha$, $\beta$), unlike SFOC which uses the ($d$, $q$) frame and requires coordinates transformation.

This paper concerns on a comprehensive comparative study between two modified DTC strategies using twelve sectors switching table and fixed switching frequency through the space vector modulation. Subsequently, the presented methods will be investigated by real-time implementation. Our control system is implemented by dSpace DS1104 signal card. This board operates with MATLAB/Simulink platform basing on TMS320F240 DSP processor.

# II. Twelve sectors switching table-DTC strategy

## II.1 Basic direct torque control strategy

Direct torque control achieves a decoupled control of the stator flux and the electromagnetic torque in the stationary frame. The control scheme of basic direct torque control strategy is shown in Fig.1

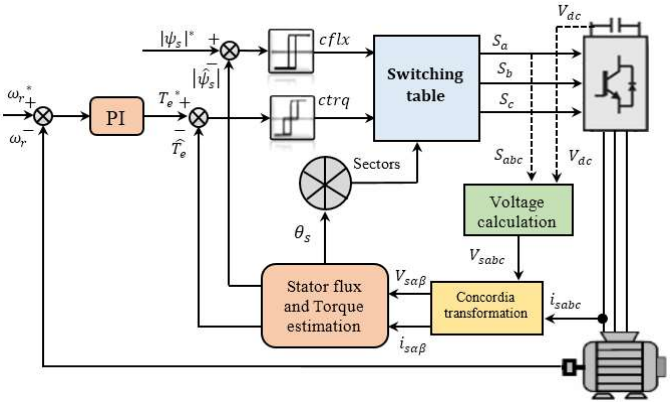


Fig.1 Block diagram of basic direct torque control algorithm

## II.2 Twelve sectors direct torque control strategy

In the conventional six sectors DTC, two switching states per sector are not considered (i.e. $V_i$ and $V_{i+3}$). This presents an ambiguity in torque control. As a proposition, the twelve sector DTC strategy divides the circular flux locus into 12 regions instead of 6 as shown in Fig.2 [6]. This makes all the six states used per sector and solves the ambiguity in torque control.

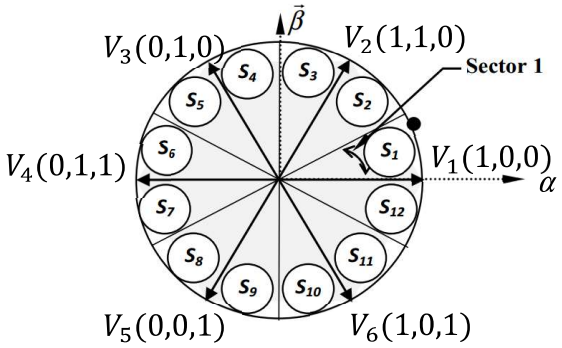


Fig.2. Voltage space vector in 12 sectors case.

In this method, the vector *V1* produces a large increase in flux and a small increase in torque for the sector *12*. On the contrary, *V2* produces a large increase in torque and small in flux. In this case, it is necessary to define small and large torque variations which requires to divide the hysteresis band of the torque into four parts instead of three. Then, all six voltage vectors can be used. The next table shows the voltage vectors of the first and the $12^{th}$ sectors, the rest sectors can be deduced in similar way [6].

**Table I: 12-Sectors Switching Table**

| | | *S1* | *S12* |
|---|---|---|---|
| **Flux** | Increase | *V1, V2* and *V6* | *V1, V2* and *V6* |
| | Decrease | *V3, V4* and *V5* | *V3, V4* and *V5* |
| **Torque** | Increase | *V2, V3* and *V4* | *V1, V2* and *V3* |
| | Decrease | *V5, V6* and *V1* | *V4, V5* and *V6* |

# III. Fixed switching frequency DTC based on SVM

## III.1 Space Vector Modulation

SVM relies on the space vector representation of the inverter output. There are no separate modulators for each phase like the conventional pulse width modulation (PWM). The reference voltages are given by space voltage vector (Fig.3). The principle of SVM is the prediction of inverter voltage vector by the projection of the reference vector $V_s^*$ between adjacent vectors corresponding to two non-zero switching states.[7], [9].

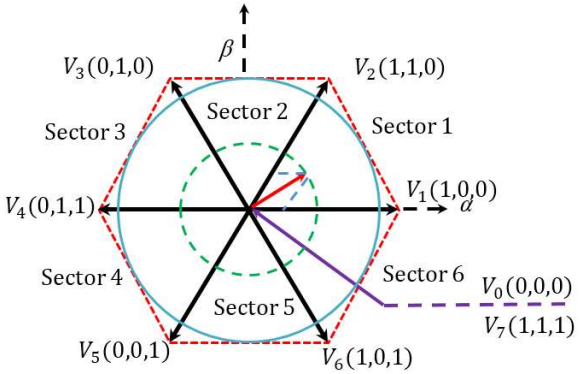


Fig.3 Diagram of voltage space vector.

The application time for each vector can be obtained by vector calculations and the rest of the time period will be spent by applying the null vector. The determination of times $T_1$ and $T_2$ corresponding to voltage vectors are obtained by simple projections:

$$T_1 = \frac{T_z}{2V_{dc}}(\sqrt{6}V_{s\beta}^* - \sqrt{2}V_{s\alpha}^*) \tag{1}$$

$$T_2 = \sqrt{2}\frac{T_z}{V_{dc}}V_{s\alpha}^* \tag{2}$$

$V_{dc}$ is DC-bus voltage.

$T_z$ is the sampling time.

The ripples in the classical DTC are affected proportionally by the width of the hysteresis bands. They still important even by reducing the bandwidths due to the discrete nature of hysteresis controller. Besides, reducing the bandwidths increases inverter switching frequency [3]. In SVM-DTC, the produced reference voltages are modulated in fixed switching frequency, this helps to reduce ripples considerably.

## III.2 SVM-DTC technique based on load angle control

The torque of the motor can be adjusted by the change of the load angle $\delta$ which is the angle between the stator and the rotor flux vectors (Fig.4). The electromagnetic torque of induction motor can be expressed in terms of stator and rotor flux vectors as follow:

$$T_e = p\frac{M_{sr}}{\sigma L_s L_r}\psi_s \times \psi_r \tag{3}$$

$$T_e = p\frac{M_{sr}}{\sigma L_s L_r}|\psi_s||\psi_r|\sin(\delta) \tag{4}$$

$\psi_s$, $\psi_r$ are stator and rotor flux vectors.

$L_s$, $L_r$ are stator and rotor inductances.

$\sigma = 1 - \frac{M_{sr}}{L_s L_r}$ is Blondel's coefficient.

$M_{sr}$ is the mutual stator-rotor inductance

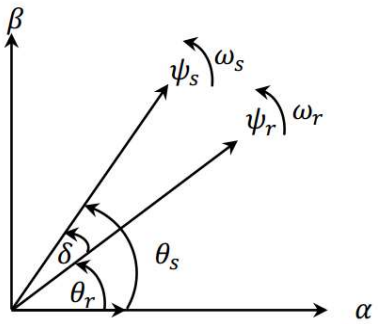


Fig.4 Stator and rotor flux vectors and angles.

The main objective of this strategy is to select voltage vector $V_s^*$ which can change $\psi_s$ then modulate it by the SVM. The produced change of the load angle by the torque controller is added to actual angle of the rotor flux vector. Then we can estimate the reference stator flux vector by the following polar-rectangular transformation formula (5)[8], [10].

$$\psi_s^* = \left|\psi_s^*\right|\cos(\delta+\theta_r) + j\left|\psi_s^*\right|\sin(\delta+\theta_r) \tag{5}$$

$\theta_s$ and $\theta_r$ are stator and rotor flux angles

The reference voltage components ($V_{s\alpha}^*, V_{s\beta}^*$) are calculated based on the stator flux error $\Delta\psi_s$ and sampling time by the following equations:

$$\begin{cases} V_{s\alpha}^* = \dfrac{\Delta\psi_{s\alpha}}{T_z} = \dfrac{\psi_{s\alpha}^* - \hat{\psi}_{s\alpha}}{T_z} + R_s i_{s\alpha} \\ V_{s\beta}^* = \dfrac{\Delta\psi_{s\beta}}{T_z} = \dfrac{\psi_{s\beta}^* - \hat{\psi}_{s\beta}}{T_z} + R_s i_{s\beta} \end{cases} \tag{6}$$

In this control scheme, the load angle $\delta$ is adjusted using PI controller. It computes the instantaneous value of slip angular frequency, this later is the time derivative of the load angle $\delta$ which required to adjust the stator flux angle [11]. The PI controller design is described in details in the reference [10]. The global diagram of load angle based DTC with space vector modulation is presented in Fig.5.

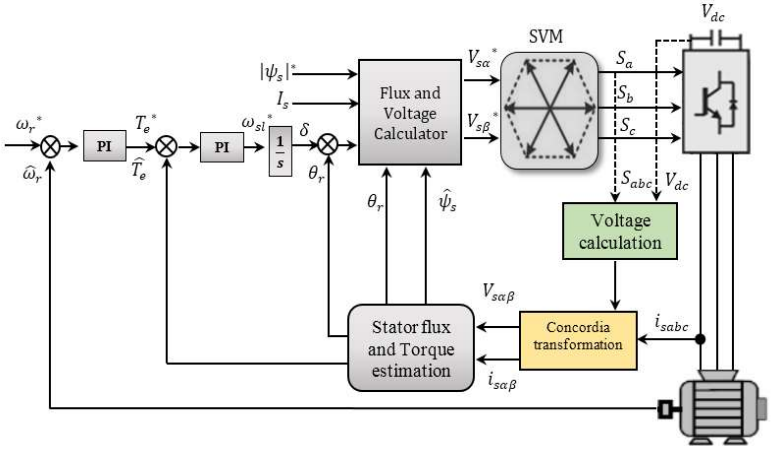


Fig.5 Block diagram of SVM-DTC technique based on load angle control.

## IV. Speed Regulation

Commonly, the tuning of PI controllers usually disregarding the physical limitation of the system such as the maximum current and voltage. In our work an anti-windup speed controller is used to enhance speed control performance by cancelling the windup phenomenon which is caused by the saturation of the pure integrator [12]. Fig.6 shows the speed anti-windup PI controller diagram block.

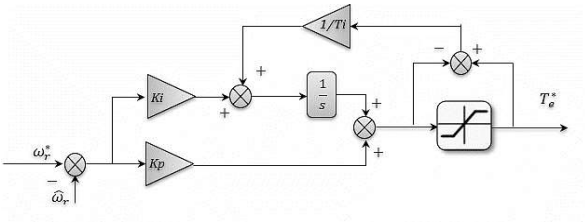


Fig.6 Speed anti-windup PI controller.

This strategy consists on the correction of the integral action based on the difference between the control signal and the saturation limit. The difference value is passed through a gain block (tracking time constant $T_i$) before arriving as feedback to the integrator.

## V. Experimental Results

The real-time implementation was done in the laboratory equipped by dSpace 1104 interface.

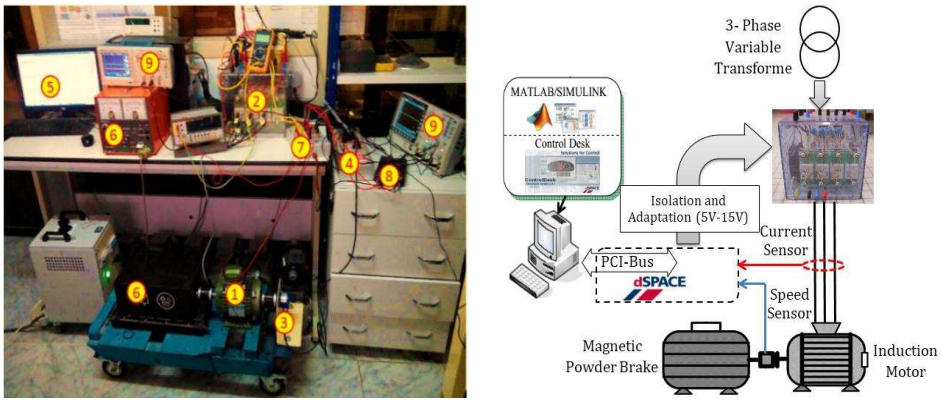


Fig.7 Presentation of the experimental setup.

The experimental test bench of IM drive is composed as presented in (Fig. 7) of: 1: A squirrel-cage IM 1.1 kW. 2: power electronics Semikron converter composed of a rectifier and an IGBT based voltage source inverter. 3: position and speed sensor (type: incremental encoder). 4: dSpace dS 1104 with 5: control desk software plugged in desk computer. 6: magnetic powder brake with load control unit. 7: Hall type current sensors. To reduce the cost of the control system, the phase voltages will be estimated from DC-bus voltage and inverter switching states (Sa, Sb, Sc) instead of use voltage sensors. 8: DC-bus voltage sensors. 9: numerical oscilloscope.

The figures below present a comparative study between the implemented DTC algorithms. The characteristics of the induction motor are given in the appendix. Different operation conditions are employed such as: starting up, steady state, load application and low speed. The figures are specified by (a) for 12 sector switching table based DTC and (b) for SVM-DTC.

### V.1 Starting up, steady state and load application

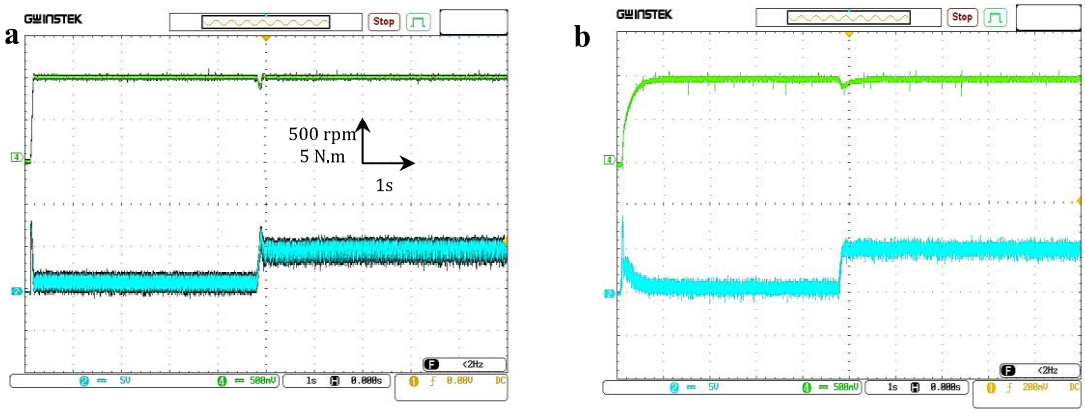


Fig.8 Rotor speed and torque responses with load application of 5 N.m.

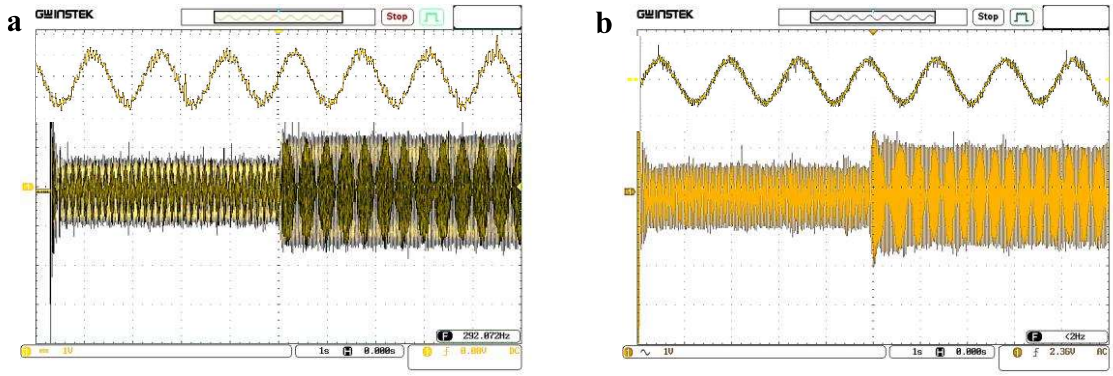


Fig.9 Stator phase current

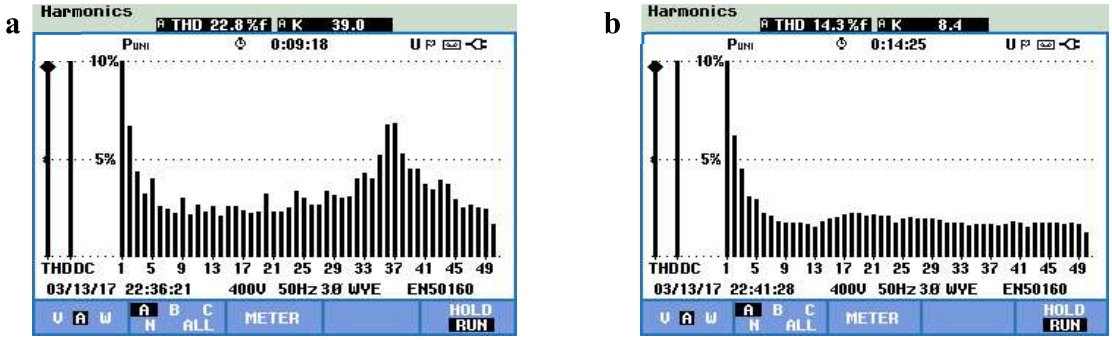


Fig. 10 Stator phase THD using power analyzer.

Fig. 8 shows the experimental results of the starting up of the motor, a load application for classical and SVM-DTC. It is clearly observed that SVM-DTC has the reducer torque ripples level. Next, in Fig.9 the stator phase current is presented. It can be seen in Fig.9(b) that the SVM-DTC shows better current waveform with less harmonics which is also verified through THD analysis in Fig.10. The SVM-DTC has lower harmonic level (14.3%) than the classical DTC (22.8%).

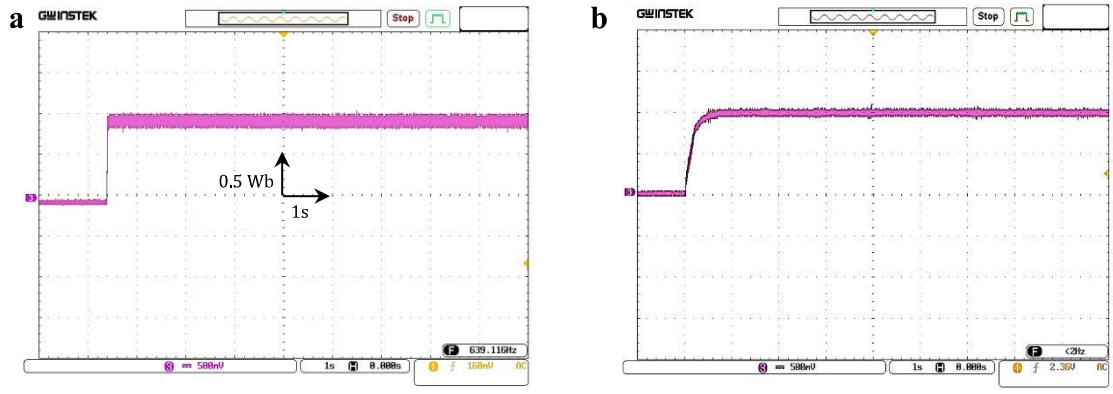


Fig.11 Stator flux magnitude.

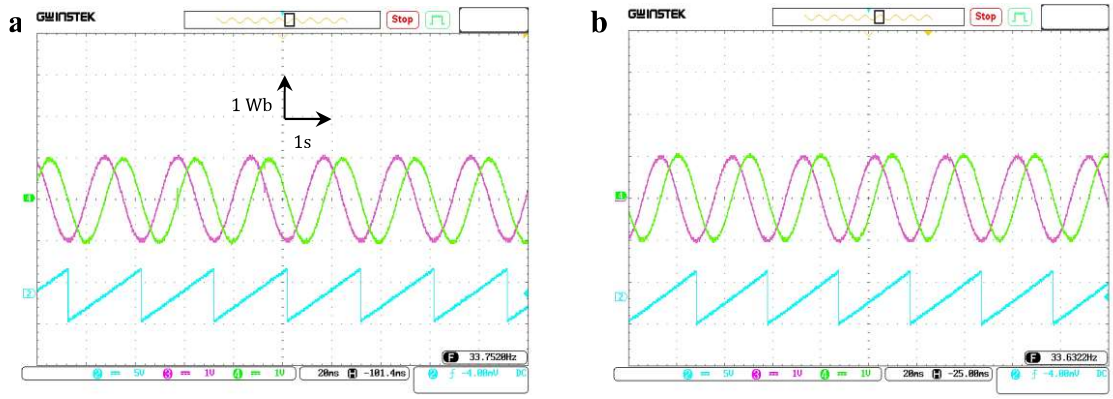


Fig.12 Stator flux axes components ($\psi_{s\alpha}$, $\psi_{s\beta}$) and position.

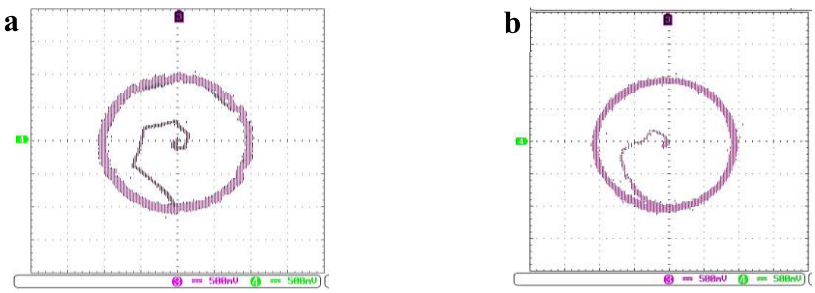


Fig.13 Stator flux circular trajectory.

Then, in Figs.11-13, the flux figures are depicted, they show flux magnitude (1div=0.5Wb), flux axes components (1div=1Wb) and circular trajectory respectively. All the presented results give a similar appearance as the simulation results. By comparing the results of Figs.11-13(a) with Figs.11-13(b) it can be seen that the flux ripples are considerably reduced in SVM-DTC.

## V.2 Low speed operation

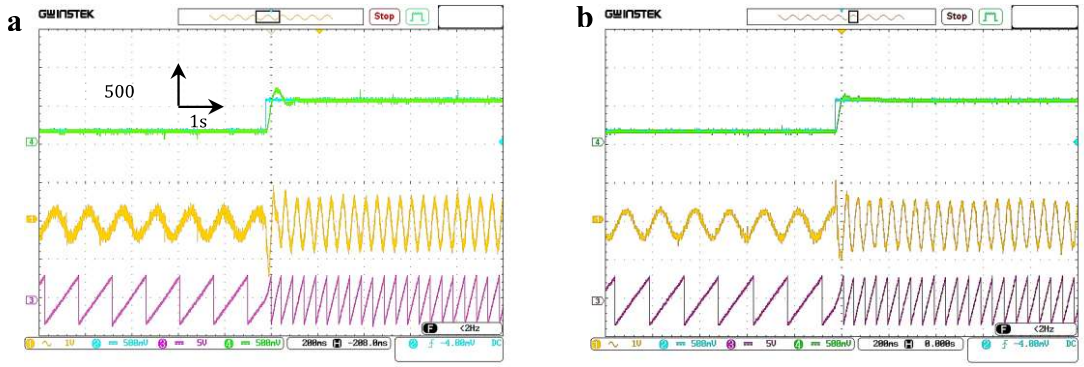


Fig.14 Low speed operation: Speed, current and flux position

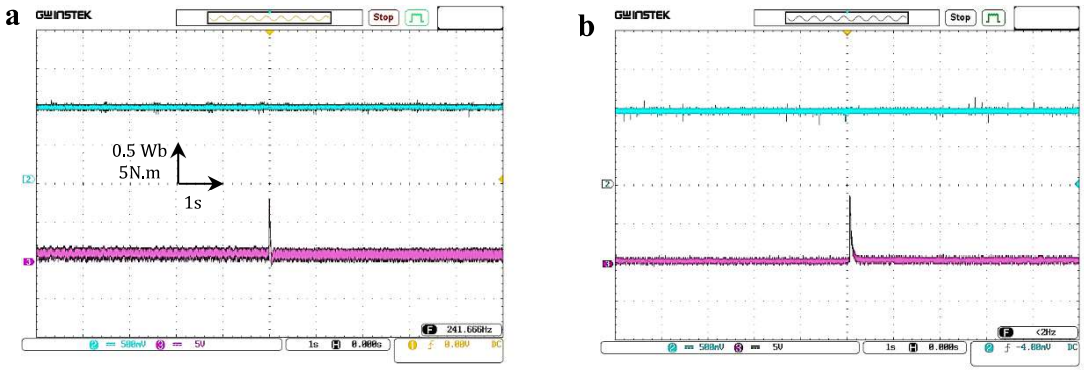


Fig.15 Low speed operation test: Flux magnitude, torque.

The low speed operation is the last considered test. It is shown in Figs.14-15 where the reference speed changes from low to medium speed regions (*200 rpm; 600 rpm*). The rotor speed shows a degraded dynamic and an inaccurate reference tracking (Fig.14). It can be seen that the rotor speed has shown some fluctuations for both control strategies. In addition, the level of current harmonics has been increased specially for the classical DTC at (*200 rpm ≈ 20.93 rad/s*) as illustrated in Fig.14(a), while the SVM-DTC kept an acceptable current waveform as presented in Fig.14(b), Then, Fig.15 presents the flux magnitude and electromagnetic torque. It is observed that the flux waveform has been deformed and the torque has been distorted. When the machine operates with low speed/frequency, the performance of DTC has been diminished. In physical explanation, at low speeds, the back-EMF decreases and the stator resistance voltage dropping cannot be longer neglected. Therefore, the accuracy of stator flux estimation becomes a major issue.

# VI. Conclusion

This paper presents comparative evaluation of two modified direct torque control method of induction motor. A conventional method based on modified switching table of twelve divisions compared to fixed switching frequency method based on load angle control and space vector modulation. The performances of control have been investigated as a comparative study by an experimental implementation using real-time interface linked to dSpace 1104.

Generally, the test results indicate that the torque and the stator flux ripples have been considerably reduced owing to the SVM use compared to switching table case. In addition, the stator phase current provides good current waveform with less harmonics. Furthermore, SVM-DTC achieves better dynamic control under different operation conditions, such as steady state, load application and low speed operation. This modified technique preserves the good proprieties of classical DTC like simple scheme designed in stationary frame. Generally, the insertion of SVM in DTC control scheme solves the most common DTC drawbacks.

# Appendix

The parameters of the three-phase Induction motor, employed for simulation and real implementation, in SI units are:

1.1kW, 50 Hz, p=2, $R_s$=6.75Ω, $R_r$=6.21Ω, $L_s$=$L_r$=0.5192 H, $M_{sr}$= 0.4957 H, $f$=0.002 SI, J=0.01240 kg.m²

# References


[1] I. Takahashi and T. Noguchi, “A New Quick-Response and High-Efficiency Control Strategy of an Induction Motor,” *Ind. Appl. IEEE Trans.*, vol. IA-22, no. 5, pp. 820–827, 1986.

[2] V. N. N, A. Panda, and S. P. Singh, “A Three-Level Fuzzy-2 DTC of Induction Motor Drive Using SVPWM,” *IEEE Trans. Ind. Electron.*, vol. 63, no. 3, pp. 1467–1479, Mar. 2016.

[3] M. Uddin and M. Hafeez, “FLC-Based DTC Scheme to Improve the Dynamic Performance of an IM Drive,” *IEEE Trans. Ind. Appl.*, vol. 48, no. 2, pp. 823–831, Mar. 2012.

[4] I. M. Alsofyani and N. R. N. Idris, “Simple Flux Regulation for Improving State Estimation at Very Low and Zero Speed of a Speed Sensorless Direct Torque Control of an Induction Motor,” *IEEE Trans. Power Electron.*, vol. 31, no. 4, pp. 3027–3035, Apr. 2016.

[5] M. Petronijevic, N. Mitroviic, V. Kostic, and B. Bankovic, “An Improved Scheme for Voltage Sag Override in Direct Torque Controlled Induction Motor Drives,” *Energies*, vol. 10, no. 5, p. 663, May 2017.

[6] R. Toufouti, S. Meziane, and H. Benalla, “Direct torque control strategy of induction motors,” *Acta Electrotech. Inform.*, vol. 7, no. 1, pp. 1–7, 2007.

[7] T. G. Habetler, F. Profumo, M. Pastorelli, and L. M. Tolbert, “Direct torque control of induction machines using space vector modulation,” *Ind. Appl. IEEE Trans.*, vol. 28, no. 5, pp. 1045–1053, 1992.

[8] J. Rodriguez, J. Pontt, C. Silva, S. Kouro, and H. Miranda, “A Novel Direct Torque Control Scheme for Induction Machines with Space Vector Modulation,” *IEEE 35th Annu. Power Electron. Spec. Conf. (IEEE Cat. No.04CH37551)*, no. 5, pp. 1392–1397, 2004.

[9] A. Ammar, A. Bourek, and A. Benakcha, “Sensorless SVM-Direct Torque Control for Induction Motor Drive Using Sliding Mode Observers,” *J. Control. Autom. Electr. Syst.*, vol. 28, no. 2, pp. 189–202, Apr. 2017.

[10] Y. Kumsuwan, S. Premrudeepreechacharn, and H. A. Toliyat, “Modified direct torque control method for induction motor drives based on amplitude and angle control of stator flux,” *Electr. Power Syst. Res.*, vol. 78, no. 10, pp. 1712–1718, 2008.

[11] A. Ammar, A. Benakcha, and A. Bourek, “Closed loop torque SVM-DTC based on robust super twisting speed controller for induction motor drive with efficiency optimization,” *Int. J. Hydrogen Energy*, pp. 1–13, Apr. 2017.

[12] M. Yang, S. Tang, and D. Xu, “Comments on “Antiwindup Strategy for PI-Type Speed Controller”,” *IEEE Trans. Ind. Electron.*, vol. 62, no. 2, pp. 1329–1332, Feb. 2015.